A General Model for Dispersed Kinetics in Heterogeneous Systems

W. John Albery,*† Philip N. Bartlett,‡ C. Paul Wilde,† and James R. Darwent⊥

Contribution from the Department of Chemistry, Imperial College, London SW7 2AY, England, and the Department of Chemistry, Birkbeck College, London WC1E 7HX, England.
Received September 25, 1984

Abstract: The kinetics of heterogeneous systems such as semiconductor electrodes, colloidal particles, oxide surfaces, and the fluorescence of dyes bound in polymer matrices or to biological membranes often give curved semilogarithmic plots when tested for first-order kinetics. However, the kinetics are not of a higher order, e.g., second, because when normalized by the initial concentration, the decay curves all lie on a common curve. It is common practice to fit such curves to a multiexponential expression. This paper presents an alternative general model, in which there is a Gaussian distribution of the logarithm of the rate constant about some mean and which introduces only one additional parameter—the width of the distribution. Data from the kinetics of semiconductors surface states, of colloidal semiconductor particles, of surface oxides, of the fluorescence decay of a dye bound to a biological membrane, and from dynamic light scattering experiments are shown to fit the model. In the case of the colloidal semiconductor particles, there is good agreement for the radial dispersion between the value found from dynamic light scattering and the value found from analysis of the kinetics.

Increasing attention is being paid to the study of the chemical kinetics of inhomogeneous systems.[1-14] In the classical homogeneous system, the usual rate laws of first- and second-order kinetics are often sufficient to explain and analyze the data. By contrast reactions taking place on surfaces, in modified electrodes, at semiconductor electrodes, in polymer matrices, and on biological membranes often do not obey simple first- or second-order kinetics. For instance, the decay of the fluorescence of the dye 6-(*p*-toluidino)-2-naphthalenesulfonate (TNS) bound to lecithin vesicles has been fitted by using an expression with up to three exponential terms.[15-17] In our own study of the illuminated p-type GaP electrode interface[18] we found, as shown in Figure 1, that the decay of the charge in the surface states exhibited "first-order" behavior in one respect; as the intensity of the light was varied, each decay curve when normalized by its initial concentration fell on a common curve. Such a normalizing procedure will not work for systems where the kinetics are higher than first order. However, in contrast to a classical homogeneous system the semilogarithmic plots in figure 1 are not linear. Because of the normalizing procedure, the nonlinearity cannot be caused by higher order kinetics. In homogeneous solution one would then conclude that the mechanism must be more complicated than a single step; models involving for instance two consecutive steps with two or more exponential terms would be invoked. These precedents have led to this type of model being applied to the analysis of the kinetics of reactions in heterogeneous systems. In a recent paper, Scott[19] has discussed the dispersion of rate constants for surface catalysis and how the distribution may be derived from analysis of the kinetics data. His model has a rather complicated distribution function involving six adjustable parameters. In this paper we present a simpler model with only two adjustable parameters and show that the model can explain kinetic data from a wide variety of different inhomogeneous systems.

The Model

Our model is a development of the "Gaussian" model we used to explain the redox behavior of the thionine/leucothionine couple in a thionine-coated electrode.[20] As the electrode potential was varied, the proportion of thionine to leucothionine in the coat on the electrode could be measured spectrophotometrically. When plotted according to the Nernst equation a good straight line was obtained, but the slope was a quarter of that expected for a two-electron transfer. We showed that this dispersion of the redox change along the potential axis could be explained if one assumed that there was a dispersion of the free energy change, ΔG^θ, according to a normal distribution, $\exp(-x^2)$, about some mean $\Delta \bar{G}^\theta$:

$$\Delta G^\theta = \Delta \bar{G}^\theta - \gamma x RT \quad (1)$$

The parameter γ describes the spread of the Gaussian distribution. When $\gamma = 0$ there is no dispersion and the system will behave in a classical homogeneous fashion.

We now develop the same model for the kinetics of heterogeneous systems, by writing an analogous equation to eq 1 for the free energy of activation.

$$\Delta G^\ddagger = \Delta \bar{G}^\ddagger - \gamma x RT \quad (2)$$

The dispersion in the first-order rate constants is then

$$k = \bar{k} \exp(\gamma x) \quad (3)$$

The most important difference between our treatment and that of Scott[19] is that we assume a Gaussian distribution in $\Delta G^\ddagger$ or in ln (k), whereas Scott's distribution function is

$$f(k) = \frac{2^{1/2} A_1 \exp[-(k - \bar{k}_1)^2/2\sigma_1^2]}{\pi^{1/2}\sigma_1 k} + \frac{2^{1/2} A_2 \exp[-(k - \bar{k}_2)^2/2\sigma_2^2]}{\pi^{1/2}\sigma_2 k}$$

† Department of Chemistry, Imperial College, London SW7 2AY, England.
‡ Department of Chemistry, University of Warwick, Coventry, Warwickshire CV4 7AL, England.
⊥ Department of Chemistry, Birkbeck College, London WC1E 7HX, England.

(1) Thomas, J. K. *Chem Rev.* **1980**, *80*, 283.
(2) Grätzel, M. *Acc. Chem. Res.* **1981**, *14*, 376.
(3) Duonghong, D.; Ramsden, J.; Grätzel, M. *J. Am. Chem. Soc.* **1982**, *104*, 2977. Moser, J.; Grätzel, M. *Ibid.* **1983**, *105*, 6547.
(4) Grätzel, M.; Frank, A. J. *J. Phys. Chem.* **1982**, *86*, 2964.
(5) Henglein, A. *Ber. Bunsenges. Phys. Chem.* **1982**, *86*, 241. Bahnemann, D.; Henglein, A.; Lilie, J.; Spanhel, L. *J. Phys. Chem.* **1984**, *88*, 709.
(6) Kuczynski, J. P.; Thomas, J. K. *Chem. Phys. Lett.* **1982**, *88*, 445. Kuczynski, J. P.; Thomas, J. K. *J. Phys. Chem.* **1983**, *87*, 5498.
(7) Kuczynski, J. P.; Milosavljevic, B. H.; Thomas, J. K. *J. Phys. Chem.* **1984**, *88*, 980.
(8) Albery, W. J.; Bartlett, P. N.; Porter, J. D. *J. Electrochem. Soc.*, in press.
(9) Prybyla, S.; Struve, W. S.; Parkinson, B. A. *J. Electrochem. Soc.* **1984**, *131*, 1587.
(10) Albery, W. J.; Calvo, E. J. *J. Chem. Soc., Faraday Trans. 1* **1983**, *79*, 2583.
(11) Albery, W. J.; Brown, G. T.; Darwent, J. R.; Saievar-Iranizad, E. *J. Chem. Soc., Chem. Commun.* submitted for publication.
(12) Darwent, J. R. *J. Chem. Soc., Faraday Trans. 1* **1984**, *80*, 183.
(13) Brown, G. T.; Darwent, J. R. *J. Chem. Soc., Faraday Trans. 1* **1984**, 1631.
(14) Brown, G. T.; Darwent, J. R. *J. Chem. Soc., Chem. Commun.*, submitted for publication.
(15) Easter, J. M.; De Toma, R. P.; Brand, L. *Biophys. J.* **1976**, *16*, 571.
(16) Dyson, R.; Isenberg, I. *Biochemistry* **1971**, *17*, 3223.
(17) Isenberg, I.; Dyson, R. *Biophys. J.* **1969**, *9*, 1337.
(18) Albery, W. J.; Bartlett, P. N. *J Electrochem. Soc.* **1982**, *129*, 2254.
(19) Scott, K. F. *J. Chem. Soc., Faraday Trans. 1* **1980**, *76*, 2065.
(20) Albery, W. J.; Boutelle, M. G.; Colby P. J.; Hillman, A. R. *J. Electroanal. Chem.* **1982**, *133*, 135.

0002-7863/85/1507-1854$01.50/0

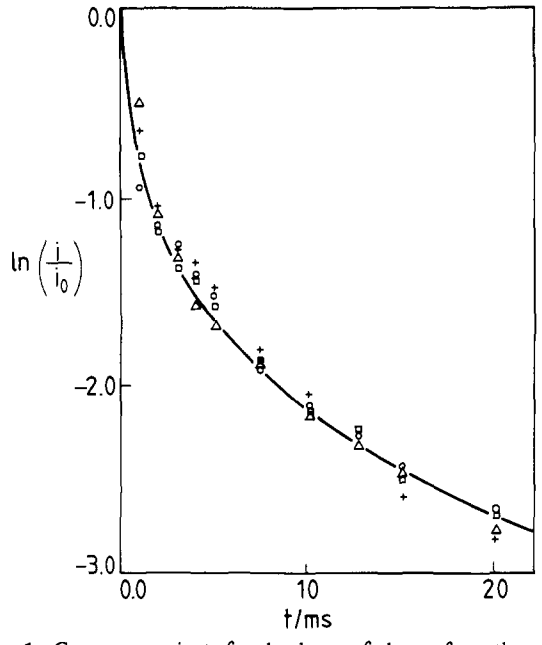

Figure 1. Current transients for the decay of charge from the surface states of illuminated p-GaP, on switching off the light. The relative irradiances were as follows: □, 1.00; Δ, 0.71; O, 0.63; +, 0.51. The curve is calculated from eq 5 with $\gamma = 2.8$.

This function has Gaussian terms in k rather than in ln (k), and also to ease subsequent integration the function has k in the two denominators. We consider that a Gaussian distribution in ln (k) is more likely to be found than one in k. A further advantage of our distribution function, which is discussed below, is the simple shifting of the function along the x axis when the distribution is modified by such factors as steady-state kinetics or radial variation.

Returning to eq 3, next we define a dimensionless time, τ, related to the mean rate constant $\bar{k}$.

$$\tau = \bar{k}t \tag{4}$$

Now integrating across the normal distribution, $\exp(-x^2)$, we find that the decay of the concentration, c, of species from their initial concentration c_0 is given by

$$\frac{c}{c_0} = \frac{\int_{-\infty}^{+\infty} \exp(-x^2) \exp[-\tau \exp(\gamma x)]\, dx}{\int_{-\infty}^{+\infty} \exp(-x^2)\, dx} \tag{5}$$

where

$$\int_{-\infty}^{+\infty} \exp(-x^2)\, dx = \pi^{1/2}$$

Note that when $\gamma = 0$, corresponding to no dispersion, eq 5 reduces to the simple first-order exponential decay

$$c/c_0 = \exp(-\tau)$$

Results

Figure 2 shows a typical three-dimensional surface calculated from eq 5. It can be seen that as the reaction proceeds the original symmetrical Gaussian becomes skewed to those species with the lower rate constants. These slower species predominate at the end, giving rise to the type of curvature seen in Figure 1.

In the Appendix we give a simple procedure for the numerical integration required for the numerator of eq 5. Results for different values of γ are plotted in Figure 3. To find a value of γ from experimental data we suggest that the ratio of $t_{7/8}$ to $t_{1/2}$ be measured where $t_{1/2}$ is the half-time of the reaction and $t_{7/8}$ is the time when one-eighth of the original reactant remains. From our results, as shown in the inset in Figure 3, we have found that

$$\gamma \approx 0.92[t_{7/8}/t_{1/2} - 3]^{1/2} \tag{6}$$

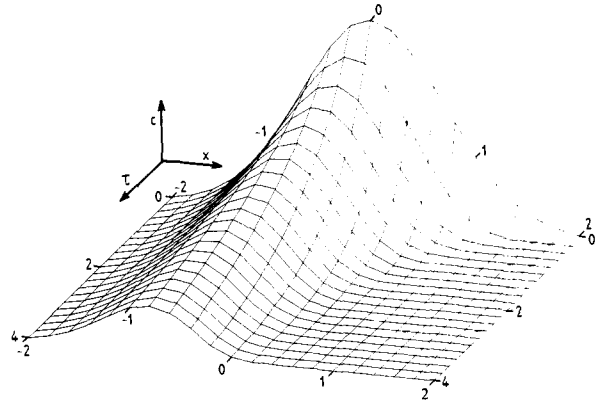

Figure 2. The decay of the Gaussian population calculated from eq 5, with $\gamma = 2$.

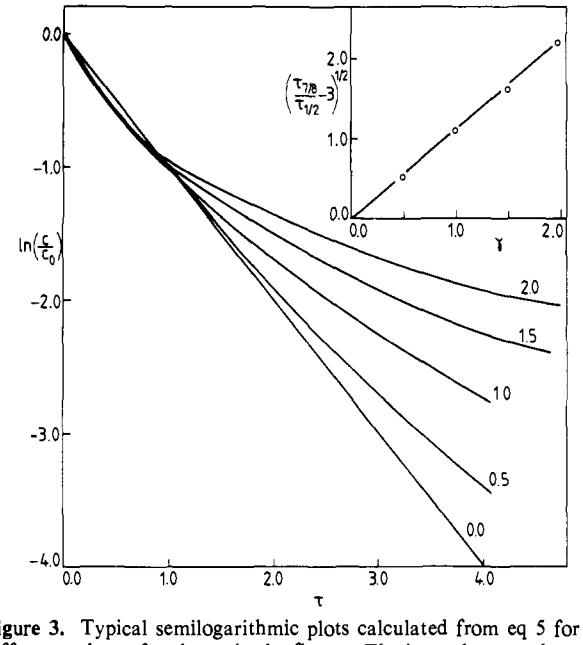

Figure 3. Typical semilogarithmic plots calculated from eq 5 for the different values of γ shown in the figure. The inset shows a plot of eq 6 which provides a convenient method of finding γ from experimental data.

The results in Figure 3 show a rough "isobestic" point at ln (c/c_0) = −1 and so for $\bar{k}$ we can write

$$\bar{k} \approx t_{1/e}^{-1} \tag{7}$$

We have also found that a useful procedure is to calculate working curves of ln (c/c_0) against ln (τ). Such a set is shown in Figure 4. Experimental data can be easily compared by plotting ln ($\lambda - \lambda_\infty$) against ln (t) where λ is some experimental measurement that is proportional to c. The experimental curve can then be matched to a theoretical curve by adjusting the displacements on both the y and x axes. An example of this procedure is given below.

Displaced Distributions

In the model presented above we have assumed that the concentration, c, obeys a Gaussian distribution $\exp(-x^2)$ centered at $x = 0$ where from eq 3 $k = \bar{k}$. In certain of the cases discussed below, the Gaussian distribution of the concentration is displaced along the x axis with respect to the point where $k = \bar{k}$. This arises, as shown in Figure 5, for instance when the population of carriers in semiconductor surface states is controlled by steady-state kinetics. There are more of those states with a longer lifetime than average and less of those with a shorter lifetime. In general, the distribution function, f, for c at $t = 0$ may not be $\exp(-x^2)$ but will be given by

$$f = \exp(p\gamma x) \exp(-x^2) \tag{8}$$

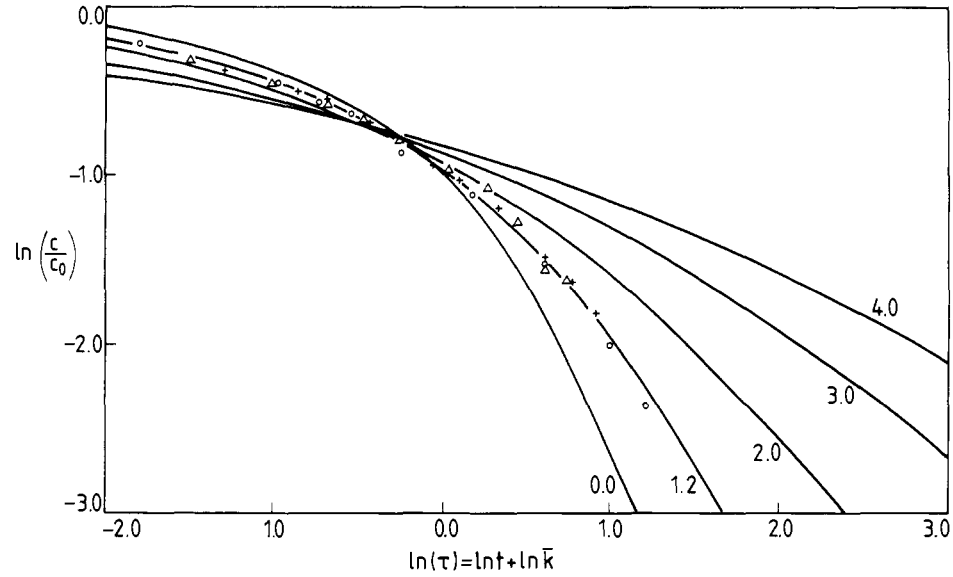

Figure 4. Typical ln/ln plots, calculated from eq 5, for different values of γ. The experimental data are typical current transients for the decay of charge from surface states of illuminated n-CdS on switching off the light, obtained at different potentials with respect to the saturated calomel electrode: +, −200 mV; Δ, −250 mV; O, −410 mV. The curve fitting the data is calculated from eq 5 with $\gamma = 1.2$. The advantage of the ln (τ) plot is that data plotted against ln (t) can be directly matched to theoretical curves.

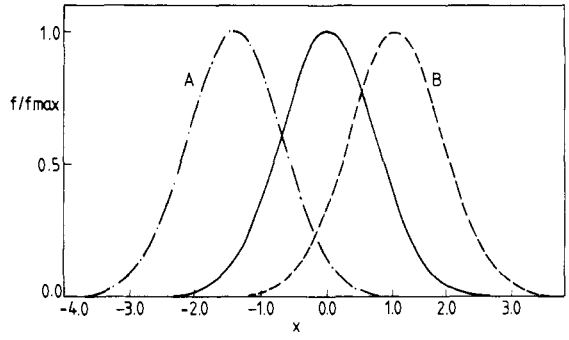

Figure 5. Typical displacements of the Gaussian distribution on the x axis. Curve A describes the GaP system where, because the surface states are populated in a steady state, the distribution favors those states which have a longer lifetime. Curve B describes the colloidal CdS system, where, because the larger particles pick up more photons, the distribution favors the faster particles with the larger area.

where p is some exponent that describes the modification to the distribution.

We can now write

$$f = \exp(p^2\gamma^2/4)\ \exp(-z^2) \tag{9}$$

where

$$z = x - p\gamma/2 \tag{10}$$

Inspection of eq 9 shows that f still has a Gaussian shape but is now centered at $z = 0$ displaced along the x axis by $p\gamma/2$. The same treatment, as presented above, will apply. The value of the dispersion parameter, γ, is unaltered. However, the value of $\bar{k}$ measured will correspond to the displaced distribution centered at $z = 0$, rather than the original distribution centered at $x = 0$. From the displacement and eq 3 we derive the following relation

$$\bar{k}_z = \bar{k}_x \exp(p\gamma^2/2) \tag{11}$$

When p is positive the distribution is displaced to include more of the faster species and $\bar{k}_z$ is larger than $\bar{k}_x$, whereas for p negative, the distribution includes more of the slower species and $\bar{k}_z$ is less than $\bar{k}_x$.

Another complication in the analysis of current transients in electrochemical systems is that the current is proportional to dc/dt as opposed to c. However, differentiation of eq 5 with respect to τ shows that the distribution is modified by a factor $\exp(\gamma x)$. Comparison with eq 8 shows that $p = 1$. In this case the faster systems make a greater contribution to the observed current. However, the retention of the Gaussian shape as it is displaced by the modifying functions is a powerful feature of the model and means that the results derived should be applicable to a wide variety of different systems. Examples are given below.

Semiconductor Surface States

Our first example is the data in Figure 1. These results were obtained as current transients on a single crystal of p-type GaP.[18] The surface is illuminated, and a negative current for the reduction of H^+ is observed. On switching the light off a transient positive current is caused by the back injection of electrons from surface states into the semiconductor.

Before the light is switched off, the population of the surface states is determined by the steady state established by the kinetics where the surface states, SS, are being populated by a flux j and are losing electrons by back injection with the dispersed rate constant, k, given by eq 3.

$$\xrightarrow{j} SS \xrightarrow{k}$$

The distribution function, $\exp(-x^2)$, will now be perturbed because there will be a higher concentration of the slower surface states compared to the faster ones. In eq 8 the value of p is −1 and, as shown in Figure 5, the maximum of the Gaussian distribution is shifted (eq 10) to $x = -\gamma/2$. However, in this case we are observing a current transient and so, as discussed above, the faster sites contribute more to the observed current with $p = 1$. Hence the two effects cancel out, and the observed $\bar{k}$ will in fact be $\bar{k}_x$.

The common curve drawn through the data in Figure 1 is calculated from eq 5 with $\gamma = 2.8$. A good fit is obtained. We have carried out similar experiments on n-type CdS. Here the transient negative current observed when the light is switched off is caused by the back injection of holes into the semiconductor. Typical data are plotted with the ln/ln procedure in Figure 4. A good fit is found with $\gamma = 1.2$.

Colloidal Semiconductors

In our studies on colloidal CdS with flash photolysis, we have found that the flash causes a transient change in the optical absorbance of the CdS.[11] We attribute this change to the separation of photogenerated holes and electrons and their trapping by surface states. Typical data for transients are plotted in Figure 6A. As with the data in Figure 1, these results have been normalized on to a common curve by dividing by the initial absorbance change. The common curve is fitted by eq 5 with $\gamma = 1.4$.

We have also studied the reduction of 1,1′-dimethyl-4,4′-bipyridinium (MV^{2+}) on TiO_2 colloid with flash photolysis.[14] The

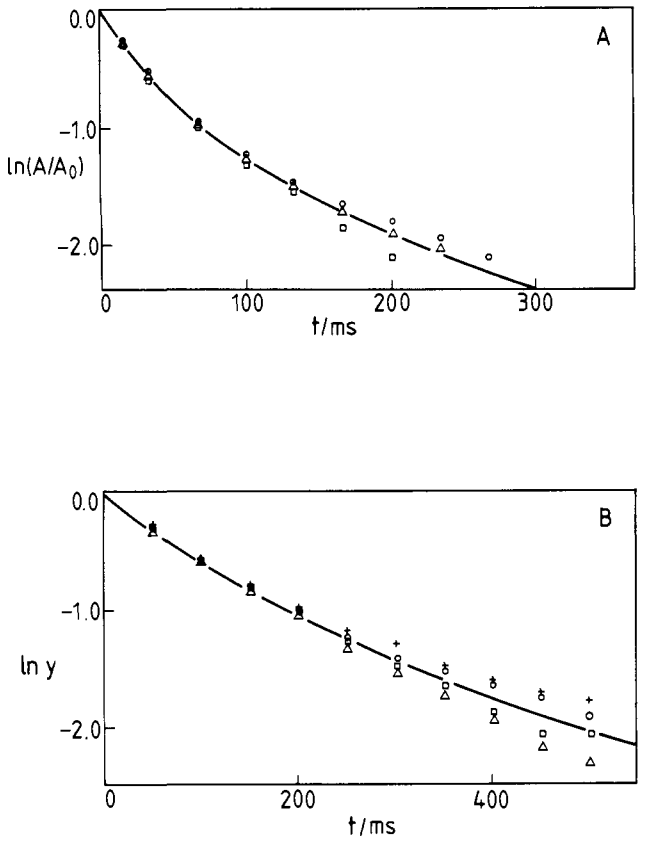

Figure 6. Typical transients for colloidal semiconductor systems. Part A shows the decay in the change of the absorbance, ΔA, after flash photolysis of CdS particles. Values of ΔA_0 were as follows: □, −0.09; Δ, −0.13; ○, −0.19. Part B shows transients for the increase in the absorbance of MV^+ in the TiO_2/MV^{2+} system where $y = (A_\infty - A)/(A_\infty - A_0)$. Values of $(A_\infty - A_0)$ were as follows: □, 0.48; Δ, 0.24; ○, 0.12; +, 0.04. The lines were calculated from eq 5 for γ equal to 1.4 and 1.1 for parts A and B, respectively.

electron-transfer reaction is followed by monitoring the absorption of the product MV^+. Figure 6B shows a set of transients this time normalized by the total amount of MV^+ formed, which in this set varied by a factor of 10. Again the data lie on a common curve which can be fitted to eq 5 with $\gamma = 1.1$.

In this example the concentration of MV^{2+} was much larger than the concentration of photogenerated electrons on the TiO_2 particles. Hence the concentration of MV^{2+} did not vary significantly and the different subpopulations of photogenerated electrons decayed by first-order kinetics. A different situation prevails when the photogenerated reactant, e.g., MV^+, is in the solution and is being oxidized on colloidal electrode particles. Here simple first-order kinetics with no dispersion are observed even though the catalytic surface may contain sites of different reactivity. This is because the decay of the MV^+ does not significantly disturb the distribution of the sites. Hence our model can only be applied to the decay of heterogeneous species under unimolecular or pseudo-first-order conditions.

The dispersion in these two examples may be caused by the same effects as seen above in the macroscopic semiconductors. Another possibility is that it is caused by variation in the size of the colloidal particles. Our work has shown that the rate of these reactions is proportional to the surface area of the particles.[14] Hence we can write for the radial distribution

$$\ln (r) = \ln (\bar{r}) + \rho x$$

giving

$$k = \bar{k} \exp(2\rho x) \qquad (12)$$

This equation has the same form as eq 3. Hence the same results will hold with

$$\gamma = 2\rho$$

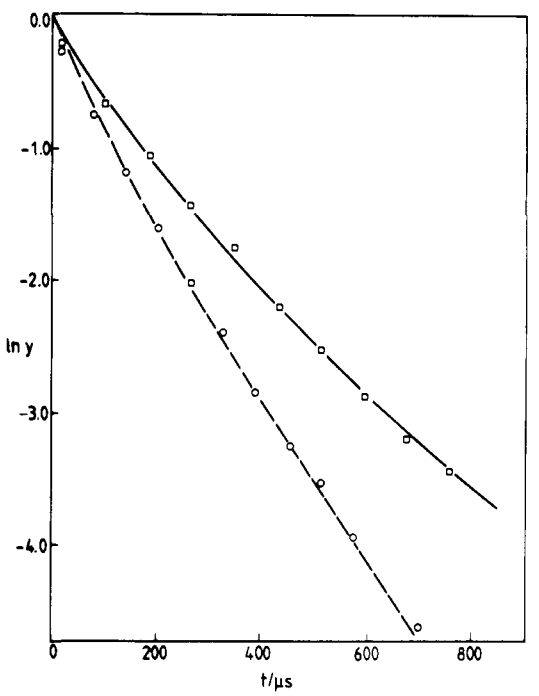

Figure 7. Decay of the autocorrelation function, $G(t)$, in dynamic light-scattering experiments for colloidal CdS (□) and for TiO_2 (○), where $y = [G(t) - G(\infty)]/[G(0) - G(\infty)]$. The lines were calculated from eq 5 for γ equal to 0.7 for CdS and to 0.6 for TiO_2.

There is a further complication in that during the flash the larger particles will capture more photons than the small ones. Hence in this case the distribution will be modified in favor of the faster particles by $(r/\bar{r})^3$ and the value of p in eq 8 will be given by

$$p = 3\rho/\gamma = 3/2$$

In collaboration with Dr Robinson we have determined the distribution of radii in the particle systems by dynamic laser light scattering.[21,22] In this method the logarithm of the autocorrelation function is plotted as a function of the delay time. The gradient of this plot is proportional to the diffusion coefficient. Typical data for our CdS and TiO_2 colloids are plotted in Figure 7. If the particles are of a uniform size, straight lines would be obtained. The deviation from the straight line is a measure of the "polydispersity" of the colloid. Various sophisticated treatments have been presented to analyze these curves.[21,23] In our view the simple Gaussian model will often be sufficient to explain the data with just the one extra parameter γ. From the Stokes–Einstein equation[24] the diffusion coefficient, D, varies with r^{-1}. Hence we find that

$$D/\bar{D} = \exp(-\rho x) \qquad (13)$$

The curves in Figure 7 are therefore analyzed by using eq 5 with $\gamma = \rho$.

The light-scattering experiment is complicated by the fact that the larger particles scattering the light more. The scattered intensity is proportional to the size of the particle or r^3. With the Gaussian model this makes no difference to the dispersion parameter, γ, but it will mean that the derived values of $\bar{D}$ and $\bar{r}$ must be corrected by using eq 11 and $p = -3$.

$$\bar{r}_x/\bar{r}_z = \bar{D}_z/\bar{D}_x = \exp(-3\gamma^2/2) \qquad (14)$$

This correction will often be significant.

Results for ρ obtained from the kinetic results described above and from the light-scattering data in Figure 7 are compared in Table I. Good agreement is found for both cases, and we may conclude first that the dispersion in the kinetic data is largely

(21) Koppel, D. E. *J. Chem. Phys.* **1972**, *57*, 4814.
(22) Brown, J. C.; Pusey, P. N.; Dietz, R. *J. Chem. Phys.* **1975**, *62*, 1136.
(23) Gardner, D. G.; Gardner, J. C.; Laush, G. *J. Chem. Phys.* **1959**, *31*, 978.

Table I. Results for the Radial Dispersion Parameter ρ

colloidal system	dynamic light scattering $\gamma = \rho$	kinetics ($\gamma = 2\rho$) γ	ρ
CdS	0.7	1.4	0.7
TiO_2	0.6	1.1	0.55

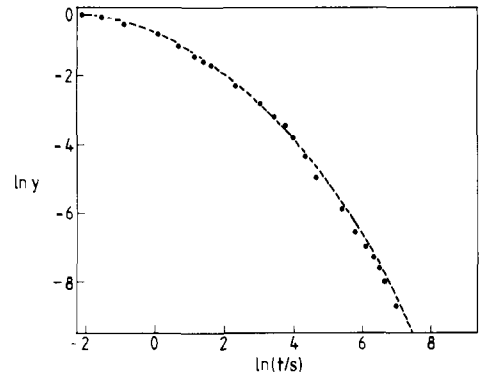

Figure 8. Current transient on a $LaNiO_3$ electrode in response to a change in electrode potential from 0.1 to 0.2 V with respect to SCE. The curve is calculated from eq 5 with γ equal to 2.4 and $y = (i_t - i_\infty)/(i_0 - i_\infty)$.

explained by the dispersion in the radii of the colloid and secondly that the Gaussian model is sufficient to analyze both the kinetic and the light-scattering data.

Surface Oxides

Another system we have found, which displays dispersed kinetics, is the Ni(II)/Ni(III) transformation in hydrated layers of $LaNiO_3$. The transformation can be followed by measuring the current transient produced by a potential step. Using the ring–disk electrode, we have shown[10] that the flux of electrons matches the flux of OH^- involved in the change of Ni(II) to Ni(III) (or vice versa) in a thin-surface zone a few monolayers thick. We had analyzed these transients with a double-exponential expression but found it difficult to suggest suitable chemical steps to explain the terms in the expression. Figure 8 shows a typical transient. The curve calculated from eq 5 with $\gamma = 2.4$ provides an excellent fit where the current has been followed to 0.07% of its initial value. Hence we conclude that this reaction consists of a single step but with dispersion.

Membrane Bound Fluorescent Probes

Our final example is typical of the use of fluorescent probes in biological membranes. Hitherto the curves describing the decay of fluorescence have been analyzed by using several exponential terms, and some authors[15] have been forced to conclude that "No theoretical significance is necessarily attached to the numerical values of the exponential parameters other than to point out that the decay kinetics are complex and require several exponential terms to obtain a good fit...." Figure 9 shows data[15] for the fluorescence decay of TNS adsorbed on single bilayer vesicles of L-α-egg lecithin. By using our model and eq 5 the data can be fitted with just the one extra parameter of $\gamma = 0.7$. We believe that the traditional application of multiexponential analysis to this type of curve may be mistaken and that our model provides a simpler and more realistic explanation.

Conclusions

The Gaussian model, presented in this paper, provides an explanation of the kinetics of heterogeneous systems where a set of

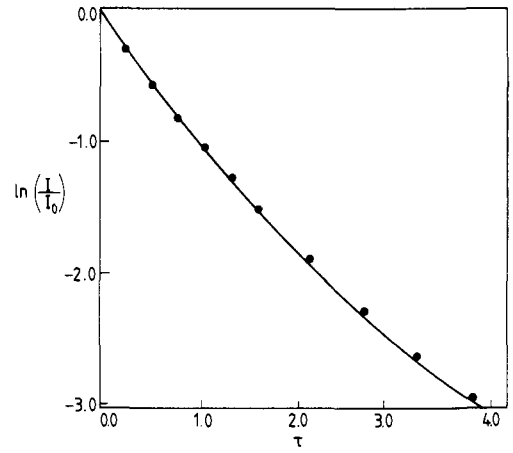

Figure 9. Decay of fluorescence intensity, I, from TNS adsorbed on lecithin. The data are from ref 15. The curve is calculated from eq 5 with $\gamma = 0.7$.

transient data when normalized fall on a common curved semilogarithmic plot. The model requires only one extra parameter, γ, which describes the dispersion of the system. We have shown that the model can be applied to semiconductor surface state kinetics, to colloidal semiconductors, to surface oxides and to fluorescence probes on membranes. In the case of the colloidal semiconductors we are able to conclude that the dispersion in the kinetic transients is caused by the dispersion in the radii. We expect this model to be widely applicable to heterogeneous systems.

Acknowledgment. We are grateful to Drs. Brian Robinson and Paul Fletcher of the University of Kent for their assistance with the dynamic light-scattering measurements. We are also grateful to Esmael Saievar-Iranizad and Graham Brown of Birkbeck College for their experimental work on the CdS and TiO_2 colloids and to Drs. Michael Lyons and Christopher Jones of Imperial College for work with $LaNiO_3$ and for assistance with Figure 2, respectively.

Appendix

In this appendix we describe a simple numerical procedure for integrating the numerator in eq 5.

$$I = \int_{-\infty}^{+\infty} \exp(-x^2)\, \exp[-\tau \exp(\gamma x)]\, dx$$

It is convenient to transform the variable by writing for $x < 0$, $x = \ln \lambda$ and for $x > 0$, $x = -\ln \lambda$. We then obtain

$$I = \int_0^1 g(\lambda)\, d\lambda$$

where

$$g(\lambda) = \lambda^{-1} \exp\{-[\ln \lambda]^2\}\{\exp[-\tau\lambda^\gamma] + \exp[-\tau\lambda^{-\gamma}]\}$$

The advantage of this transformation is that the integration limits are now 0 and 1 rather than $\pm\infty$.

The integration can be conveniently carried out by using the extended Simpson's rule[25]

$$I = (0.2/3)\{2[g(0.1) + g(0.3) + g(0.5) + g(0.7) + g(0.9)] + g(0.2) + g(0.4) + g(0.6) + g(0.8) + e^{-\tau}\}$$

(24) Robinson, R. A.; Stokes, R. H. "Electrolyte Solutions"; Butterworths: London, 1959; p 12.
(25) Abramowitz, M.; Stegun, I. A. "Handbook of Mathematical Functions"; Dover: New York, 1965; p 886.